

Catalytic Two-Electron Reductions of N₂O and N₃[−] by Myoglobin in Surfactant FilmsMekki Bayachou,[†] Lhadi Elkbir,[‡] and Patrick J. Farmer^{*,†}

Department of Chemistry, University of California, Irvine, California 92697-2025, and Faculté des Sciences, Université Chouaib Doukkali, El Jadida, Morocco

Received June 10, 1999

Myoglobin (Mb), in films of dimethyldidodecylammonium bromide (ddab) on graphite electrodes, is used as a catalyst to mediate the electrochemical reduction of nitrous oxide (N₂O) as well as the isoelectronic ion azide (N₃[−]) in aqueous solutions. The electrocatalytic reductions are characterized by a rate-dependent irreversibility in cyclic voltammograms of Mb/ddab in the presence of the substrates. Bulk electrolysis shows that the reduction of ¹⁵N¹⁵NO by Mb/ddab yields ¹⁵N¹⁵N as shown by GC/MS. The catalytic reduction of azide results in almost quantitative formation of ammonia. These electrocatalytic processes are rationalized as two-electron reductions, with the catalyst cycling between the Fe(I) and Fe(III) states of Mb. To our knowledge, this is the first characterization of N₂O reduction by an Fe porphyrin or heme protein.

Introduction

Nitrous oxide, popularly known as laughing gas, is a greenhouse gas and one of many causes of ozone depletion.¹ The widespread use of nitrogen-based fertilizers, coupled with incomplete bacterial denitrification, has been suspected to be an important source of the recent global increase in atmospheric N₂O.^{2,3} The complete denitrification pathway consists of a chain of individual steps carried out by separate enzymes within denitrifying bacteria, eq 1.^{4,5}



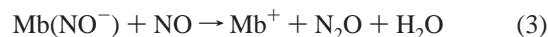
The reduction of N₂O to N₂, carried out by nitrous oxide reductases, N₂ORs, is the last step of this process. The thermodynamically downhill reduction of N₂O to N₂ is used as an independent respiratory process by certain anaerobic bacteria.^{5,6}

The catalytic centers of native N₂ORs known to date are almost exclusively copper-based. However, enzymes containing other metals at their catalytic sites have also been shown to reduce N₂O. The FeMo cofactor of nitrogenase and the cobalamin-dependent methionine synthase are two striking examples.⁷ The Cu-containing N₂OR from *Wolinella succinogenes* contains an Fe heme suggested to be a part of a dinuclear Cu heme catalytic center.^{5,8,9} Though its role in the catalysis is

controversial, the heme does seem to be obligatory for the activity of this enzyme.^{9a}

Our previous investigations on dissimilatory denitrification reactivity utilized myoglobin (Mb) to model the heme-catalyzed reductions of nitrite and nitric oxide.^{10,11} Nassar and Rusling discovered that the electrochemical response of Mb increases by more than 3 orders of magnitude when it is incorporated into a multilayer film of a surfactant, such as dimethyldidodecylammonium bromide (ddab), on a pyrolytic graphite electrode surface.^{12,13} The aqueous electrochemistry of these Mb/ddab films resembles that of Fe porphyrins in organic solvents in that both Fe^{III/II} and Fe^{II/I} couples are chemically accessible and reversible. But aqueous-phase ligands readily interact with the Fe site in Mb/ddab, as demonstrated by shifts in Mb/ddab reduction potentials and Soret band energies in their presence.¹⁴

We have used this system to study the chemical mechanisms involved in denitrification. In the case of nitrite, we reported that electrocatalytic reduction by Mb/ddab yields NO, N₂O, and N₂ as gaseous products, eq 2.¹⁰



We recently showed that nitric oxide reduction by Mb/ddab results in nitrous oxide via the reaction of nitroxyl (NO[−]) myoglobin with NO, eq 3.¹¹ The present work addresses the

[†] University of California.[‡] Université Chouaib Doukkali.

- (1) (a) Dickinson, R. E.; Cicerone R. J. *Nature* **1986**, *319*, 109–115. (b) Cicerone, R. J. *J. Geophys. Res.* **1989**, *94*, 18216. (c) Badr, O.; Probert, S. D. *Appl. Energy* **1993**, *44*, 197. (d) Crutzen, P. J. *Atmospheric Chemical Processes of the Oxides of Nitrogen, Including Nitrous Oxide*; John Wiley & Sons: New York, 1981; pp 17–44.
- (2) Troglor, W. C. *Coord. Chem. Rev.* **1999**, *187*, 303–327.
- (3) Averill, B. A. *Chem. Rev.* **1996**, *96*, 2951.
- (4) Payne, W. J. *Denitrification*; John Wiley & Sons: New York, 1981.
- (5) Zumft, W. G. *Microbiol. Mol. Biol. Rev.* **1997**, *61*, 553.
- (6) McEwan, A.; Greenfield, A. J.; Wetstein, H. G.; Jackson, J. B.; Ferguson, S. J. *J. Bacteriol.* **1985**, *164*, 823.
- (7) (a) Liang, J.; Burris, R. H. *J. Bacteriol.* **1989**, *171*, 3176. (b) Drummond, J. T.; Matthews, R. G. *Biochemistry* **1994**, *33*, 3732. (c) Drummond, J. T.; Matthews, R. G. *Biochemistry* **1994**, *33*, 3742.
- (8) Teragushi, S.; Hollocher, T. C. *J. Biol. Chem.* **1989**, *264*, 1972.

- (9) (a) Zhang, C.-S.; Hollocher, T. C.; Kolodziej, A. F.; Orme-Johnson, W. H. *J. Biol. Chem.* **1991**, *266*, 2199. (b) Farrar, J. A.; Zumft, W. G.; Thomson, A. J. *Proc. Natl. Acad. Sci. U.S.A.* **1998**, *95*, 9891.
- (10) Lin, R.; Bayachou, M.; Greaves, J.; Farmer, P. J. *J. Am. Chem. Soc.* **1997**, *119*, 12689.
- (11) Bayachou, M.; Lin, R.; Cho, W.; Farmer, P. J. *J. Am. Chem. Soc.* **1998**, *120*, 9888.
- (12) (a) Rusling, J. F.; Nassar, A.-E. F. *J. Am. Chem. Soc.* **1993**, *115*, 11897. (b) Nassar, A.-E. F.; Bobbitt, J. M.; Stuart, J. D.; Rusling, J. F. *J. Am. Chem. Soc.* **1995**, *117*, 10986. (c) Nassar, A.-E. F.; Zhang, Z.; Hu, N.; Rusling, J. F.; Kumosinski, T. E. *J. Phys. Chem.* **1997**, *101*, 2224.
- (13) Nassar, A.-E. F.; Willis, W. S.; Rusling, J. F. *Anal. Chem.* **1995**, *67*, 2386.
- (14) Farmer, P. J.; Lin, R.; Bayachou, M. *Comments Inorg. Chem.* **1998**, *20*, 101.

catalytic reduction of N_2O on Mb/ddab electrodes leading to N_2 and may be relevant to the mechanism of reduction of N_2O in *W. succinogenes* N_2OR .

Experimental Section

Materials. Myoglobin from horse skeletal muscle was purchased from Sigma and purified using published literature procedures.¹³ The concentration of myoglobin in solution after purification was estimated by visible spectroscopy. ddab was purchased from Acros. All other chemicals were reagent grade. Nitrous oxide (N_2O) was purchased from Air Gas.

^{15}N -labeled nitrous oxide was prepared by oxidation of ^{15}N -labeled hydroxylamine in the presence of Fe^{III} and stored in a U-tube cooled with liquid nitrogen. A sample of freshly prepared $^{15}N^{15}NO$ was transferred to a homemade IR cell (ZnO windows) to check its purity by IR spectroscopy on a Mattson GYGNUM IR spectrometer. ^{15}N -labeled hydroxylamine was obtained from Isotec Inc.

Pyrolytic graphite (PG) was purchased from Union Carbide. Homemade electrodes were prepared by sealing 0.4 cm diameter cylinders of PG in a glass tube body using epoxy, leaving exposed basal plane disks as the electrode active surface. Contacts with electrical wires were made with silver paste. Nanopure water with a specific resistance greater than 18 $M\Omega$ cm was provided by a Barnstead Nanopure system.

Mb/ddab Film Preparation. A sample of ddab (0.046 g) was suspended in 15 mL of water. The mixture was ultrasonicated for at least 6 h until the solution became clear. A 10 μ L portion of 0.01 M ddab and 10 mL of a 0.5 mM solution of metMb (Fe^{III}) were cast onto the surface of each basal-plane-oriented PG electrode. The myoglobin/ddab-modified electrodes were allowed to stand overnight in a closed vessel and then dried in open air for at least 12 h.

UV-vis spectra were recorded using a Hewlett-Packard 8453 spectrometer. Films were prepared on quartz slides in the same way that the actual electrodes were prepared. Dried slides were immersed in anaerobic pH 7 solution, in a three-necked quartz cuvette. N_2O was introduced by bubbling; other substrates were dissolved in the solution. The reduced deoxy Mb was formed by anaerobic reduction with either dithionite or sodium borohydride.

Electrochemistry. A BAS 100W electrochemical system was used, and a standard three-electrode cell was adopted, consisting of a platinum wire counter electrode, a saturated calomel reference electrode (SCE), and a PG disk working electrode. All electrochemical experiments were performed at room temperature (22 ± 2 °C). The electrodes were immersed in solutions containing 0.1 M NaBr electrolyte. To work under an anaerobic atmosphere, the analyte solution was purged with purified nitrogen for at least 20 min prior to the beginning of each series of electrochemical experiments. A positive pressure of nitrogen was maintained over the solution throughout the experiments. N_2O substrate was introduced into the electrochemical cell via a switching three-way gas line. N_2O was bubbled through the aqueous solution, and a positive pressure of N_2O was maintained in a closed electrochemical cell.

Bulk electrolysis was carried out on larger basal-plane-oriented PG thin electrodes ($1.0 \times 2.5 \times 0.1$ cm) coated with Mb/ddab on the two sides, in an airtight multiarmed electrochemical cell. Controlled potential was applied to the PG electrodes using a BAS 100W workstation and a BAS PWR-3 power module. The working (PG plate) and reference (SCE) electrodes were immersed in the same analyte solution, while the counter electrode, a Pt grid, was separated from the main compartment by a fine frit.

Product Analysis. Colorimetric assay methods were used to detect N-based products. Ammonia was quantified using the indophenol reaction, with a detection limit of ca. 2 μ M under the conditions of our analysis.^{16a,b} For detection of nitrite and hydroxylamine, procedures were followed as described in refs 16c and 16d, respectively.

For mass spectroscopy experiments, the same multiarmed airtight electrochemical cell, used in bulk electrolysis, was connected via fused

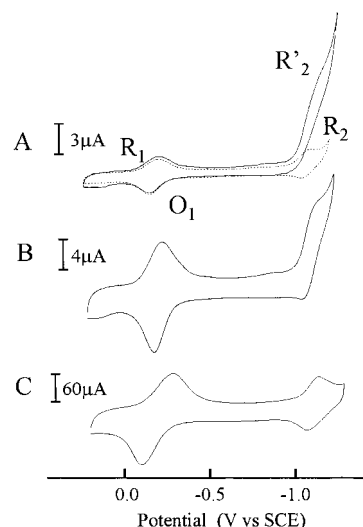


Figure 1. Cyclic voltammograms of Mb/ddab in the absence (···) and presence (—) of substrate N_2O at (A) 20 mV/s, (B) 0.2 V/s, and (C) 5 V/s.

silica lines to a Micromass Autospec mass spectrometer through a GC interface. In a continuous mode, the headgas during the bulk electrolysis was continuously transferred to the mass spectrometer using a He purge. In a sampling mode, the headgas was sampled in a loop and transferred into the mass spectrometer via the GC interface through a Plot GC column (fused silica 50 m \times 0.32 mm, Al_2O_3/KCl coating), using a mixture of He/106 ppm of Ar as a carrier gas. Data were acquired in the EI mode at 1000 resolution.

Prior to mass spectrometry/bulk electrolysis experiments, $^{15}N^{15}NO$ was prepared as described under Materials, under a He atmosphere, and stored in a U-tube cooled with liquid nitrogen. The U-tube containing the labeled $^{15}N^{15}NO$ was mounted in parallel with the carrier gas line using a three-way stopcock. To transfer the labeled gas into the electrochemical cell, the carrier gas was switched to pass through the U-tube. The latter was taken out of the liquid nitrogen and gently warmed on the sides to transfer some of the solid N_2O into the gas phase.

Results

Catalytic Reduction of N_2O . The electrochemical response of Mb immobilized in ddab on PG electrodes, in the absence and presence of N_2O , is shown in Figure 1. In the absence of substrate N_2O , two successive one-electron reversible waves are observed. The first wave, R_1 , is assigned to the reduction of Fe^{III} to Fe^{II} of the heme group of Mb.^{12,13} The second wave, R_2 , corresponds to the reduction of Fe^{II} to the Fe^I state.¹² Under an atmosphere of N_2O , while no change occurs at the level of Fe^{III}/Fe^{II} redox couple, a significant change is observed at the potential of the second wave (Figure 1A): the addition of N_2O causes an increase in current, I_c , of the Fe^{II}/Fe^I redox couple, wave R'_2 , indicating multiple electron transfer per iron site, along with a concomitant loss of reversibility. Increasing the scan rate gradually restores the reversibility of the Fe^{II}/Fe^I couple, while the ratio of the measured current, I_c , to the current in the absence of N_2O , I_0 , decreases (Figure 1B,C). In the absence of Mb catalyst on ddab-coated electrodes, the reduction of N_2O is not observed before solvent reduction.

(16) (a) Liu, M.; Costa, C.; Moura, I. *Methods Enzymol.* **1994**, *243*, 303. (b) Searcy, R. L.; Simms, N. M.; Foreman, J. A.; Bergquist, L. M. *Clin. Chim. Acta* **1965**, *12*, 170. (c) Jeffery, G. H.; Bassett, J.; Mendham, J.; Denney, R. C. *Vogel's Textbook of Quantitative Chemical Analysis*, 5th ed.; Longman Scientific & Technical: London, 1989; p 702. (d) Frear, D. S.; Burrell, R. C. *Anal. Chem.* **1955**, *27*, 1664.

(15) Cotton, F. A.; Wilkinson, G. *Advanced Inorganic Chemistry*, 6th ed.; John Wiley & Sons: New York, 1999; p 323.

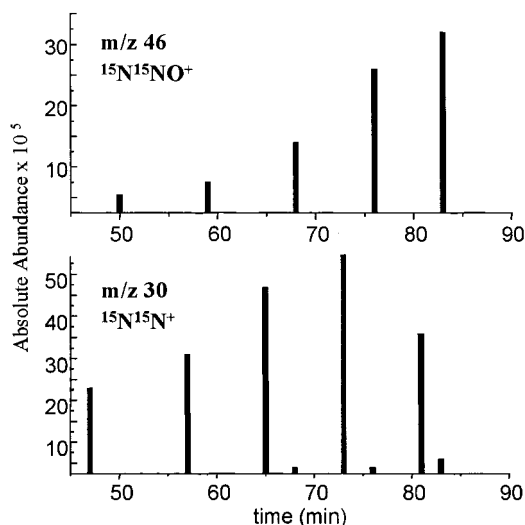


Figure 2. GC/MS of headgas over the electrolyzed $^{15}\text{N}^{15}\text{NO}$ solution on Mb/ddab sampled during bulk electrolysis and separated at room temperature on an $\text{Al}_2\text{O}_3/\text{KCl}$ -coated silica line.

To identify the products of the reduction, saturated aqueous solutions of doubly labeled N_2O was reduced at potentials corresponding to wave R'_2 and the headgas is sampled at different times during the bulk electrolysis into a mass spectrometer through a GC interface. Large PG plates coated with a film of Mb/ddab are used as working electrodes at pH 7. The electrolysis is run at a potential of ca -1.1 V/SCE. The gases from the electrochemical cell are sampled into a fused-silica line coated with $\text{Al}_2\text{O}_3/\text{KCl}$ before transfer to the mass spectrometer.

Figure 2 shows the GC/MS response of the sampled aliquots of the headgas as the electrolysis proceeds. The peaks at $m/z = 46$ and $m/z = 30$, after injections at different times during the bulk electrolysis, correspond to $^{15}\text{N}^{15}\text{NO}^+$ and $^{15}\text{N}^{15}\text{N}^+$, respectively. At $m/z = 30$, each injection of a sample of the headgas gives rise to two peaks. The small peak coming at the same time as the peak at $m/z = 46$ ($^{15}\text{N}^{15}\text{NO}^+$) is the fragmentation product ($^{15}\text{N}^{15}\text{N}^+$) of the parent ion, occurring in the mass spectrometer chamber. The other major peak, coming earlier, corresponds to $^{15}\text{N}^{15}\text{N}$ originating from the headgas of the electrochemical cell. No aqueous N-based products, such as ammonia, were detected after bulk electrolysis of N_2O to the detection limits of our method.

Catalytic Reduction of Azide. Figure 3 shows the electrochemical response of Mb/ddab electrodes in the presence of 11 mM NaN_3 . The formal potential of the $\text{Fe}^{\text{III}}/\text{Fe}^{\text{II}}$ couple shifts by 98 mV to more negative potentials. At slow scan rates, a large current increase is observed at negative potentials giving rise to wave R''_2 . Increasing the scan rate decreases the current of wave R''_2 and eventually restores the normal current response of the second couple of Mb/ddab. Bulk electrolysis of azide solutions at -1.1 V/SCE on Mb/ddab electrodes shows formation of ammonia as an aqueous product of the electrocatalysis, as determined by a standard colorimetric assay.¹⁶ Measurement of the current passed during two electrolysis experiments gave ratios of 2.1 and 2.3 electrons per ammonia produced.

Discussion

The voltammetric response of Mb/ddab is unusual in that both the $\text{Fe}^{\text{III}}/\text{Fe}^{\text{II}}$ and $\text{Fe}^{\text{II}}/\text{Fe}^{\text{I}}$ couples are accessible in buffered aqueous solutions.^{10–14} In the presence of N_2O or N_3^- , there is a large current increase concomitant with loss of reversibility (Figures

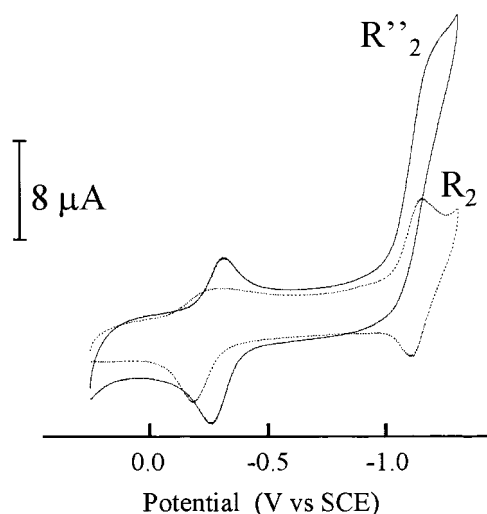


Figure 3. Cyclic voltammograms of Mb/ddab in the absence (···) presence (—) of 11 mM azide in a pH 7 buffer (scan rate 100 mV/s).

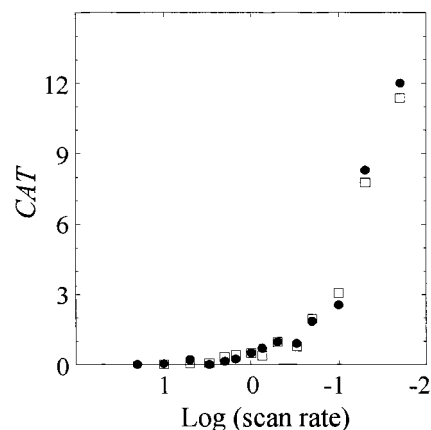


Figure 4. Plot of CAT vs $\log(\text{scan rate, V/s})$. CAT, as defined in the text, is the ratio $(I_c - I_0)/I_0$. Data points were obtained from two sets of experiments in saturated N_2O solutions at pH 7.

1 and 3), consistent with an electrocatalytic process at the formal potential of the $\text{Fe}^{\text{II}}/\text{Fe}^{\text{I}}$ redox couple. The loss of reversibility indicates that the reductive catalysis is driven by an irreversible reaction of $\text{Fe}^{\text{I}}(\text{Mb})$ with the corresponding substrate. The catalytic turnover can be measured by the change in catalytic current CAT, defined as $(I_c - I_0)/I_0$. Data for N_2O reduction by Mb/ddab are shown in Figure 4 as a logarithmic function of the scan rate. The observed CAT is larger at slow scan rates, decreases as the scan rate is increased, and eventually falls to zero at scan rates above a few volts per second.

The first reduction wave, R_1 , is not affected by the presence of substrate N_2O , as N_2O does not bind to either Fe^{III} or Fe^{II} states of Mb/ddab, Figure 1. Likewise, no shift is seen in the Soret absorbance of either oxidation state in the presence of N_2O . In the presence of azide, a significant negative shift for the $\text{Fe}^{\text{III}}/\text{Fe}^{\text{II}}$ redox potential is observed, indicative of azide binding to the Fe^{III} heme center, Figure 3. For azide solutions, the Soret shifts indicate binding to the Fe^{III} but not the Fe^{II} state of Mb. Thus, neither substrate binds to Fe^{II} Mb and both catalytic reactions are due to interactions of the substrate with the Fe^{I} state of Mb/ddab.

To understand this reactivity, we carried out bulk electrolyses of N_2O on Mb/ddab electrodes and looked for solution and gaseous products. In $^{15}\text{N}^{15}\text{NO}$ -saturated aqueous solutions, a strong signal corresponding to $^{15}\text{N}^{15}\text{N}$ (as determined by GC/MS) was observed during the bulk electrolysis at the Fe^{I}

Scheme 1

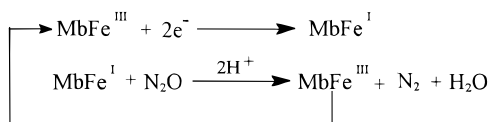
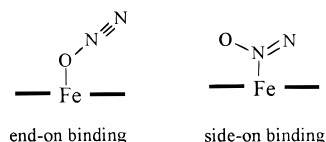
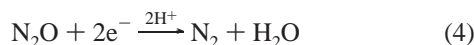


Chart 1



potential, Figure 2. This catalysis mimics the behavior of the N_2ORs enzymes, which reduce nitrous oxide by two electrons, yielding dinitrogen and water, eq 4. We cannot confirm the formation of water H_2O during this catalysis, but no ammonia or other N-based aqueous products were detected by standard analytical procedures. The formation of ammonia during the analogous electrocatalytic reduction of azide provides added evidence of such a two-electron reactivity, eq 5; in this case the ammonia formation was almost quantitative with the current passed.



These results also explain the formation of N_2 in the reduction of nitrite by Mb/ddab, which proceeds after the primary gaseous product, N_2O , builds up in the headgas.¹⁰ Younathan et al. reported similar N_2 formation during nitrite reductions catalyzed by polymerized porphyrins, via a proposed bimolecular coupling of nitrido complexes.¹⁷ Such bimolecular coupling is unobtainable with Mb/ddab.

The uncatalyzed reduction of N_2O , yielding N_2 and water, is highly exergonic but kinetically slow. Neutral N_2O is linear in its ground state, but the one-electron-reduced product, N_2O^- , is predicted to adopt a bent structure.¹⁸ Therefore, a high kinetic barrier arises during the first electron transfer. As a result, the electrochemical reduction of N_2O on bare metal electrodes occurs only at very negative potentials.¹⁹ Studies have implied that these reductions proceed via the intermediacy of adsorbed hydrogen or metal oxides that partially overcome the high energy barrier of the first electron transfer. In our case, this limiting barrier may be avoided through a two-electron pathway utilizing the Fe^{I} and Fe^{III} oxidation states of the Mb/ddab catalyst, Scheme 1, in which there is a direct reaction between the catalyst and substrate.

The reaction of N_2O with the Fe^{I} catalyst may be considered through either an end-on or a side-on coordination, Chart 1. It is well-known that N_2O can react with transition metal complexes forming the corresponding oxo derivatives along with N_2 evolution.^{20–24} For example, the stoichiometric reaction of N_2O with a divalent Cr(II) porphyrinogen complex results in

Scheme 2

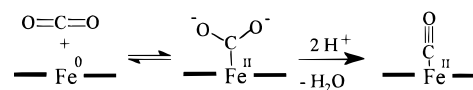


Table 1. Catalytic Efficiencies for Mb/Ddab Reductions of N-Oxide Substrates^a

	nitrite (NO_2^-)	nitric oxide (NO)	nitrous oxide (N_2O)
concn (mM)	12	1.93 ^b	31 ^b
I_s/I_0	60	90	9
efficiency ($\text{M}^{-1} \text{s}^{-1}$)	500	4600	29

^a Conditions: currents from linear-sweep voltammograms at 20 mV/s in pH 7 buffer, using equivalent Mb/ddab electrodes. ^b Saturated solutions of the gases.²⁶

an oxo-Cr(IV) product.²⁰ In our system, reduction of an O-bound adduct would result in an $\text{Fe}^{\text{III}}-\text{OH}$ species and N_2 . Alternatively, an interaction may occur between Fe^{I} and the central nitrogen of N_2O . Semiempirical calculations on N_2O have shown that the LUMO is largely localized on the central nitrogen atom, with the HOMO localized on the terminal oxygen and nitrogen atoms.^{18b} The two-electron reduction of CO_2 by a highly reduced Fe^0 porphyrin catalyst has been suggested to occur via a transient carbenoid species, $\text{Fe}^{\text{II}}-\text{CO}_2^{2-}$, Scheme 2, which loses water to form an iron(II) carbonyl.²⁵

The overall efficiencies of Mb/ddab in reductive catalysis of N-oxide substrates are given in Table 1, but in all cases, the electrocatalytic currents observed are affected by substrate depletion within the surfactant film.^{26,27} Under steady-state conditions, where the concentration of the substrate remains in large excess over that of the catalyst, the expected sigmoidal catalytic current wave is never obtained in any of the Mb/ddab-catalyzed reductions, even down to the slowest scan rates used (5 mV/s).^{10,11,14} The absence of steady-state behavior is likely a consequence of the biphasic (surfactant/water) nature of the medium; close to the electrode surface, the catalysis depletes the substrate concentration within the film and replenishment from the bulk solution is slow in comparison.²⁶ Still, we believe the order of relative efficiencies, $\text{NO} > \text{NO}_2^- > \text{N}_2\text{O}$, in Table 1 represents an inherent catalytic reactivity and not the variable effect of substrate depletion.

Conclusion

We have characterized the electrocatalytic reductions of isoelectronic N_2O and N_3^- by Mb/ddab in aqueous solutions. To our knowledge, this is the first characterization of N_2O reduction by an Fe porphyrin or heme protein. Using ¹⁵N labeling, we have characterized the production of N_2 gas during N_2O reduction, whereas azide reduction has been shown to produce ammonia almost quantitatively with the current passed,

- (17) Younathan, J. N.; Wood, K. S.; Meyer, T. J. *Inorg. Chem.* **1992**, *31*, 3280.
 (18) (a) Ferguson, E. E.; Fehsenfeld, F. C.; Schmeltekopf, A. L. *J. Chem. Phys.* **1967**, *47*, 3085. (b) Rabalais, J. W.; McDonald, J. M.; Scherr, V.; McGlynn, S. P. *Chem. Rev.* **1971**, *71*, 73. (c) Hopper, D. G.; Wahl, A. C.; Wu, R. L. C.; Tiernan, T. O. *J. Chem. Phys.* **1976**, *65*, 5474. (d) Bardsley, J. N. *J. Chem. Phys.* **1969**, *51*, 3384.
 (19) (a) Kudo, A.; Mine, A. *J. Electroanal. Chem. Interfacial Electrochem.* **1996**, *408*, 267. (b) Kudo, A.; Mine, A. *Appl. Surf. Sci.* **1997**, *121/122*, 538.

- (20) Dionne, M.; Jubb, J.; Jenkins, H.; Wong, S.; Gambarotta, S. *Inorg. Chem.* **1996**, *35*, 1874.
 (21) Bottomley, F.; Lin, J. B. I.; Mukaida, M. *J. Am. Chem. Soc.* **1980**, *102*, 5238.
 (22) Vaughan, G. A.; Rupert, P. B.; Hillhouse, G. L. *J. Am. Chem. Soc.* **1987**, *109*, 5538.
 (23) Tan, S. A.; Grant, R. B.; Lambert, R. M. *J. Catal.* **1987**, *104*, 156.
 (24) Groves, J. T.; Roman, J. S. *J. Am. Chem. Soc.* **1995**, *117*, 5594.
 (25) Bhugun, I.; Lexa, D.; Savéant, J.-M. *J. Am. Chem. Soc.* **1996**, *118*, 1769.
 (26) (a) Savéant, J.-M.; Su, K. B. *J. Electroanal. Chem. Interfacial Electrochem.* **1984**, *171*, 341. (b) Andrieux, C. P.; Hapiot, P.; Savéant, J.-M. *Chem. Rev.* **1990**, *90*, 723.
 (27) (a) Weiss, R. F.; Price, B. A. *Mar. Chem.* **1980**, *8*, 347. (b) IUPAC. *Solubility Data Series*; Young, C. L., Ed.; Pergamon Press: Oxford, England, 1981; Vol. 8.

by eq 5. Both catalytic transformations are rationalized as proceeding through a two-electron reduction step, between accessible Fe^I and Fe^{III} states of the catalyst. These results partially explain the formation of N₂ observed in our previous investigation regarding the biomimetic nitrite reduction on Mb/ddab electrodes. The single-site transformation of N₂O to N₂ by Mb is likely different from that occurring at the dinuclear Cu N₂OR enzymes but may be relevant to the catalytic reduction of N₂O in *W. succinogenes* reductase. Our present results show that, if accessible in biological systems, an Fe^I heme center may react directly with N₂O.

Acknowledgment. We thank Dr. John Greaves for valued help with the mass spectral experiments, Dr. Don Blake for the use of a PLOT GC column, and Dr. Barbara Finlayson-Pitts for help in the characterization of ¹⁵N¹⁵NO. This work was supported by the National Science Foundation (Grant CHE-9702332), the Petroleum Research Fund (Grant PRF-31804-G3), and startup funding from the University of California, Irvine. M.B. thanks the IDB for postdoctoral support.

IC990672U